AD-A235 968

‖‖‖‖‖‖‖‖‖‖‖‖‖‖‖‖

TECHNICAL REPORT NO. 6

Nonexponential Solvation Dynamics of Simple Liquids and Mixtures

Wlodzimierz Jarzeba, Gilbert C. Walker, Alan E. Johnson
and Paul F. Barbara

In Press

in

Chemical Physics

University of Minnesota
Department of Chemistry
Minneapolis, MN 55455

May 6, 1991

This statement should also appear in Item 10 of the Document Control Data–DD
Form 1473. Copies of the form available from cognizant grant of contract adminstrator.

DTIC ELECTE MAY 1 5 1991 C

Accession For	
NTIS GRA&I	☑
DTIC TAB	☐
Unannounced	☐
Justification	

By___
Distribution/
Availability Codes
Dist | Avail and/or Special
A-1

DTIC FILE COPY

91 5 14 030

REPORT DOCUMENTATION PAGE	Form Approved OMB No. 0704-0188

1a REPORT SECURITY CLASSIFICATION Unclassified	1b RESTRICTIVE MARKINGS

2a SECURITY CLASSIFICATION AUTHORITY	3. DISTRIBUTION/AVAILABILITY OF REPORT Approved for public release distribution unlimited
2b. DECLASSIFICATION/DOWNGRADING SCHEDULE	

4 PERFORMING ORGANIZATION REPORT NUMBER(S) Technical Report No. 6	5. MONITORING ORGANIZATION REPORT NUMBER(S)

6a. NAME OF PERFORMING ORGANIZATION Department of Chemistry University of Minnesota	6b OFFICE SYMBOL (If applicable)	7a. NAME OF MONITORING ORGANIZATION Office of Naval Research

6c. ADDRESS (City, State, and ZIP Code) 207 Pleasant St. SE Minneapolis, MN 55455	7b. ADDRESS (City, State, and ZIP Code) Chemistry Program 800 North Quincy St. Arlington, VA 22217

8a. NAME OF FUNDING/SPONSORING ORGANIZATION Office of Naval Research	8b. OFFICE SYMBOL (If applicable)	9 PROCUREMENT INSTRUMENT IDENTIFICATION NUMBER N0014-89-J-1746

8c. ADDRESS (City, State, and ZIP Code) Chemistry Program, 800 N. Quincy St. Arlington, VA 22217	10 SOURCE OF FUNDING NUMBERS			
	PROGRAM ELEMENT NO	PROJECT NO.	TASK NO	WORK UNIT ACCESSION NO.

11. TITLE (Include Security Classification)
Nonexponential solvation dynamics of simple liquids and mixtures

12. PERSONAL AUTHOR(S)
Wlodzimierz Jarzeba, Gilbert C. Walker, Alan E. Johnson and Paul F. Barbara

13a TYPE OF REPORT Technical	13b TIME COVERED FROM TO	14. DATE OF REPORT (Year, Month, Day) May 6, 1991	15 PAGE COUNT

16 SUPPLEMENTARY NOTATION

17 COSATI CODES			18 SUBJECT TERMS (Continue on reverse if necessary and identify by block number)
FIELD	GROUP	SUB-GROUP	

19 ABSTRACT (Continue on reverse if necessary and identify by block number)
Novel measurements on the microscopic solvation dynamics of coumarin probes in several simple polar solvents and solvent mixtures have been made using the time dependent fluorescence Stokes shift technique. The microscopic solvent relaxation function, C(t), is observed to be poorly modeled by a single exponential decay in many cases. The average exerimental solvation times,   , for pure solvents and binary solvent mixtures are close to values predicted by dielectric continuum theory. The results suggest that molecular motion of solvent molecules near the solute can be responsible for microscopic solvation components of C(t) that are not predicted using bulk dielectric data of the neat solvent and the dielectric continuum theory. In addition to the solvation dynamics results, some potential sources of probe molecule non-ideality are examined, and it is shown that these effects are not significant contributors to experimental error for (CONTINUED)...

20 DISTRIBUTION/AVAILABILITY OF ABSTRACT ☒ UNCLASSIFIED/UNLIMITED ☐ SAME AS RPT ☐ DTIC USERS	21 ABSTRACT SECURITY CLASSIFICATION Unclassified
22a NAME OF RESPONSIBLE INDIVIDUAL Dr. Ronald A. De Marco	22b TELEPHONE (Include Area Code)	22c OFFICE SYMBOL

DD Form 1473, JUN 86   Previous editions are obsolete.   SECURITY CLASSIFICATION OF THIS PAGE

S/N 0102-LF-014-6603   Unclassified

19.

(abstract continued) these C(t) measurements.

Nonexponential solvation dynamics of simple liquids and mixtures

Wlodzimierz Jarzeba[1], Gilbert C. Walker, Alan E. Johnson and Paul F. Barbara

Department of Chemistry, University of Minnesota, Minneapolis, MN 55455, USA

Novel measurements on the microscopic solvation dynamics of coumarin probes in several simple polar solvents and solvent mixtures have been made using the time dependent fluorescence Stokes shift technique. The microscopic solvent relaxation function. $C(t)$, is observed to be poorly modeled by a single exponential decay in many cases. The average experimental solvation times. $\langle \tau_s \rangle$, for pure solvents and binary solvent mixtures are close to values predicted by dielectric continuum theory. but in many cases, the observed $C(t)$ shape does not agree with that predicted by dielectric continuum theory. The results suggest that molecular motion of solvent molecules near the solute can be responsible for microscopic solvation components of $C(t)$ that are not predicted using bulk dielectric data of the neat solvent and the dielectric continuum theory. In addition to the solvation dynamics results, some potential sources of probe molecule non-ideality are examined, and it is shown that these effects are not significant contributors to experimental error for these $C(t)$ measurements.

1. Introduction

Time resolved fluorescence spectroscopy of polar fluorescent "probes" that have a dipole moment that depends significantly upon electronic state have recently been extensively used to measure microscopic solvation dynamics in a broad range of solvents. The fundamentals of this field. and recent results from several groups. have been extensively reviewed [1–3]. Major progress on transient solvation has recently been made as the result of new ultrafast spectroscopic methods and a number of novel theoretical approaches. The basic experiment is as follows:

(1) Ultrashort optical excitation of an equilibrated ground (S_0) state probe/solvent system produces an electronically excited (S_1) probe surrounded by a nonequilibrium solvent configuration.

(2) After excitation. the solvent configuration relaxes towards the new equilibrium configuration for the S_1 state of the probe. giving rise to a time dependent fluorescence Stokes shift.

This shift is monitored and analyzed to quantify the solvation dynamics via the function $C(t)$, which is defined by eq. 1.

[1] Permanent address: Faculty of Chemistry. Jagiellonian University, 3 Karasia. 30-060 Kracow. Poland.

$$C(t) = \frac{\bar{\nu}(t) - \bar{\nu}(\infty)}{\bar{\nu}(0) - \bar{\nu}(\infty)} \qquad (1)$$

Here $\bar{\nu}(0)$, $\bar{\nu}(t)$, $\bar{\nu}(\infty)$ represent the frequency of the intensity maximum of the fluorescence spectrum of the probe immediately after photon excitation. at some time. t, after excitation. and at a time sufficiently long to ensure that the solvent configuration has reached equilibrium.

In the last few years. the first $C(t)$ measurements of the solvation dynamics of ordinary, non-viscous room temperature liquids have been made using state of the art (subpicosecond and femtosecond) fluorescence spectrometers [4–6]. In addition to a few representative polar aprotic solvents, such as propionitrile [7–8], the solvation dynamics of water was measured for the first time [9]. At the same time, theoretical activity on microscopic solvation dynamics has blossomed [10–20]. In addition to the importance of $C(t)$ data in the study of the microscopic solvation dynamics of polar solutes. the data have been used indirectly in modeling ultrafast electron transfer reactions, such as the excited state intramolecular electron transfer of bianthryl [21].

Theoretical treatments of microscopic solvation dynamics have gone considerably beyond the traditional Debye uniform dielectric continuum model.

with additional effects including non-spherical probe cavities, non-uniform dielectric response of the solvent, and non-Debye relaxation dynamics of the solvent. The potential role of translational diffusion of the solvent near the probe has been investigated by continuum theories and with other approaches. Another theoretical approach, the linearized mean spherical approximation (MSA) model for solvation, considers certain aspects of the molecularity of solvation explicitly, but still allows for analytical evaluation. The most explicitly molecular view of solvation dynamics is found in the molecular dynamics simulations of various model probes in water and other solvents.

Theoretical interpretation of experimental $C(t)$ data is an active area of research despite the limited number of measurements that are available for common solvents. One obstacle in making thorough interpretations has been the existence of ultrafast decay components in $C(t)$ which are experimentally difficult to resolve. Nevertheless, a number of theoretical issues have been raised. The apparent deviation, in certain cases, between experimental $C(t)$ curves and the predictions of the dielectric continuum model (which employs bulk dielectric data $\epsilon(\omega)$ to characterize the solvent) has been used as evidence for the importance of "molecularity" of the solvent. One important point of view that has received a lot of attention is the so-called Onsager "inverted snowball" model, which has been realized quantitatively by the MSA treatment of solvation. Qualitatively, this model, which emphasizes rotational reorientation of the solvent, predicts that the solvent polarization contribution from the small number of solvent molecules (dipoles) near the probe relaxes considerably slower than the contribution due to the bulk-like liquid far from the probe [15–16]. Two additional molecular effects that have been discussed are translational diffusion of solvent molecules near the probe and the librational motion of solvent molecules or fragments of solvent molecules (e.g. frustrated rotations of hydroxyl groups).

In this paper we further investigate these issues in the study of microscopic solvation dynamics by reporting and analyzing the $C(t)$ function for several previously unstudied solvents. We also present ultrafast measurements of $C(t)$ for a binary solvent mixture. Finally, we explore the potential non-ideality of coumarin probes due to intramolecular charge transfer in S_1, and, in particular, electron transfer involving twisted intramolecular charge transfer states [22].

2. Experimental

Coumarin 152 and coumarin 153 were obtained from Exciton Inc. and used without further purification. For the various coumarin experiments, the concentration of the probe was $\approx 10^{-4}$ molar. Reagent grade benzonitrile (Aldrich) was purified by vacuum distillation from P_2O_5. The other solvents (reagent or spectroscopic grade) were found to be free of fluorescent impurities and were used without further purification.

Coumarin 152   Coumarin 153
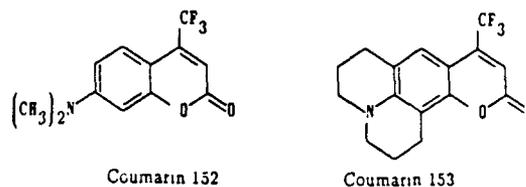
Time and wavelength resolved emission transients were recorded with a femtosecond fluorescence up-conversion apparatus that has been described in detail elsewhere [4]. The apparatus has a 280 femtosecond (fwhm) instrument response function. Briefly, the laser source is a linear, 2-jet femtosecond dye laser (Styryl 8 gain, HITCI saturable absorber, 792 nm, 70 fs) that is synchronously pumped by the second harmonic of an actively mode-locked Nd:YAG laser (Quantronix 416). The dye laser output is amplified at an 8.2 kHz repetition rate by seven passes through a thick dye jet (Styryl 8) that is optically pumped by a copper vapor laser. The sample solution is excited by the second harmonic of the amplified dye laser at 396 nm (≈ 130 fs, ≈ 0.3 μJ) which travels through a variable delay stage. The fluorescence from the sample is combined with the residual 792 nm light in a KDP crystal to generate the sum frequency (fluorescence upconversion). The fluorescence transients in this paper correspond to plots of the intensity of the sum frequency light (at a specific emission wavelength) versus the optical delay of the excitation pulse.

Time resolved emission data in the nanosecond

range were measured by time correlated single photon counting using an apparatus described previously [23].

3. Results and discussion

3.1. Methods of data analysis

Extensive new data on the transient solvation of coumarins are presented in this paper. The experiments are an in depth application of the approach we recently described [7–8]. Two experimental schemes are used to measure the solvation relaxation function. $C(t)$, specifically, the spectral reconstruction and the "linear wavelength" techniques. The former method is simpler to understand but requires much

more instrumental time. The spectral reconstruction method requires several fluorescence versus time transients. $I(t, \lambda)$, measured at various fluorescence wavelengths. λ. Via a convolution procedure involving the known instrument response function, the individual transients are each fit to a model multiexponential function which represents the ideal response of the probe to an instantaneous (delta function) excitation. An example of typical fluorescence transients are shown in fig. 1 for the fluorescent probe coumarin 153 in propylene carbonate.

After calibrating the data for the instrument sensitivity as a function of wavelength, the multiexponential representations of the fluorescence dynamics are combined to construct emission spectra at various times after excitation. The time dependent fluorescence frequency maximum. $\bar{\nu}(t)$, is obtained by fitting the spectrum at each time. t, to a standard empirical functional form for broad spectra, namely the log-normal function. This procedure (spectral reconstruction) was developed by Maroncelli and Fleming [24].

Time dependent fluorescence spectra for coumarin 153 in propylene carbonate are displayed in fig. 2. The experimental points are plotted along with the log-normal function fits (lines). The shifting toward lower frequency (longer wavelength) is clearly ob-
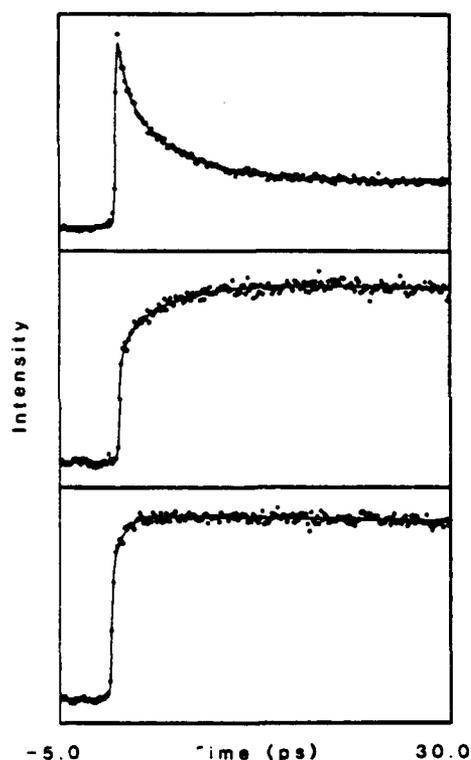
Fig. 1. Fluorescence transients of coumarin 153 in propylene carbonate at room temperature obtained using the fluorescence upconversion technique. The upper box shows the fluorescence at 483 nm. the middle box shows fluorescence at 581 nm. and the lower box shows fluorescence at 537 nm.
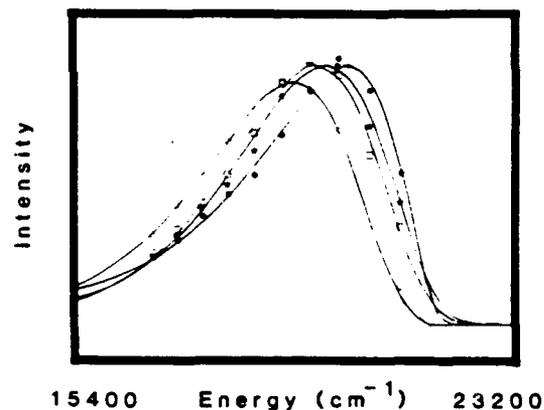
Fig. 2. Time-dependent fluorescence spectra of coumarin 153 in propylene carbonate obtained using the transients in fig. 1 (and several others at different wavelengths) and the spectral reconstruction technique. The solid lines are log-normal fits to the data points which are denoted with ● (0.1 ps). ★ (0.5 ps). ☐ (1.0 ps) and ○ (5.0 ps).

Experimental solvation parameters for simple solvents at 298 K. τ_1 and τ_2 are the time constants of a biexponential fit to the transient solvation data. $C(t)$. $\langle \tau_s \rangle$ is the average solvation relaxation time. C152 corresponds to coumarin 152 and C153 corresponds to coumarin 153. lw is linear wavelength and se is spectral reconstruction

Solvent	Probe	Method	τ_1 (ps)	τ_2 (ps)	$\langle \tau_s \rangle$ (ps)
Propylene carbonate	C152 [a]	sr	0.43 (46%)	4.1 (54%)	2.4
	C152 [a]	lw	0.64 (58%)	4.8 (42%)	2.4
	C153	sr	0.48 (50%)	6.2 (50%)	3.4
	C153	lw	0.60 (40%)	4.6 (60%)	3.0
Methanol	C152 [a]	sr	1.16 (40%)	9.57 (60%)	6.21
		lw	1.26 (60%)	8.35 (40%)	4.10
Propanol	C153	sr	14 (30%)	40 (70%)	33
		lw	20 (30%)	63 (70%)	31
DMSO	C152	lw	0.33 (57%)	2.3 (43%)	1.2
	C153	lw	0.33 (44%)	2.2 (56%)	1.4
Acetone	C152	lw	0.31 (47%)	0.99 (53%)	0.67
		or	0.70 [b]	–	0.70
	C153	lw	0.83	–	0.83
DMF	C152	lw	0.40 (55%)	1.7 (45%)	1.0
	C153	lw	0.75 (55%)	2.5 (45%)	1.5
		or	1.4 [b]	–	1.4
Acetonitrile	C152	lw	0.27 (73%)	1.05 (27%)	0.48
		or	0.56	–	0.56
Propionitrile	C152 [a]	sr	0.31 (48%)	1.34 (52%)	0.85
		lw	0.33 (68%)	1.50 (32%)	0.70
Benzonitrile	C152	lw	2.3 (49%)	8.2 (51%)	5.3
			4.7	–	4.7
Water	DMACAA [c]	sr	0.16 (33%)	1.2 (67%)	0.86
	C343 [d]	sr	0.25 (50%)	0.96 (50%)	0.61

[a] Ref. [8].

[b] For this case observed solvation dynamics can be expressed reasonably well also by single exponential decay.

[c] DMACAA – sodium salt of the 7-dimethylaminocoumarin-4-acetic acid, ref. [9].

[d] Coumarin 343, ref. [6].

served in the data. The $C(t)$ data are parameterized in this paper by fitting the $\bar{\nu}(0)$, $\bar{\nu}(t)$, and $\bar{\nu}(\infty)$ values obtained from the log-normal fits, to a model biexponential decay function. The amplitudes and relaxation times for the two exponential components of $C(t)$ for a number of solvents are shown in table 1 and discussed below.

The alternative "linear wavelength" method, which only requires a single fluorescence transient for the measurement of $C(t)$, is based on two assumptions. First, the procedure is most accurate when the loss of excited state population is negligibly small during the

solvation process. This is the situation for the experiments described in this paper, as the average solvation time $\langle \tau_s \rangle$ is on the order of a few picoseconds and the excited state lifetimes of the various probes are on the order of nanoseconds.

The second assumption is associated with the dependence of the spectral shape on the emission maximum, $\bar{\nu}$. It is assumed that the *dependence* of the emission shape on $\bar{\nu}(t=\infty)$ (which can be measured by static spectroscopy in different solvents) is the same as the dependence of the emission shape on $\bar{\nu}(t)$ during the solvation process in a single solvent

wavelength can be found for which the emission intensity (see below) is directly proportional to the frequency of the fluorescence maxima. then the emission dynamics at this wavelength (the "linear wavelength") offer a direct measure of $C(t)$.

The correct linear wavelength for a particular probe is determined by plotting the spectral density $k_n^0(\nu) g(\nu)$ versus $\bar{\nu}(t=\infty)$ for various emission frequencies. $\nu_k k_n^0(\nu)$ is the radiative rate constant and $g(\nu)$ is the normalized emission shape. These quantities can be measured by combining static emission data and lifetime data in various solvents. The emission frequency. ν. for which $k_n^0(\nu) g(\nu)$ is directly proportional to $\bar{\nu}(t=\infty)$ is the linear wavelength. For coumarin 153. the linear wavelength is 480 nm. More details on this procedure can be found elsewhere [3].

3.2. A summary of the C(t) measurements

All available room temperature femtosecond measurements of solvation dynamics for different solvents. including many new results. are summarized in table 1. The results presented in table 1 were in many cases obtained using both the spectral reconstruction method and the linear wavelength approach. It can be seen from the table that solvation dynamics is generally nonexponential. The data can be reasonably well represented by biexponential fits. However. we believe that this is only one of the possible representations of generally nonexponential solvation dynamics. Low-temperature measurements show that in many cases the biexponential representation of the data has to be replaced by triexponential functions. see below. The two relaxation times presented in table 1 differ in some cases (propylene carbonate. methanol) by almost an order of magnitude. On the other hand. for some solvents (acetone. DMF. propanol) these two times differ only by a factor of three. In these cases. the difference between the quality of monoexponential and biexponential fits can be very small and biexponential (or nonexponential) behavior can only be decided by careful analysis of the residuals of fitted functions. In such doubtful cases we present both exponential and biexponential representations of the data. although a biexponential fit is always better than a single exponential fit. It can be seen from the data that both the spectral reconstruc-

lar results. The presented values of relaxation times and average solvation times for the same probe and solvent differ less than 20%. This 20% value seems to be a reasonable estimate of our error in this experiment regardless of the method used to study solvation dynamics. Differences between the results obtained with different probe molecules. coumarin 152 and coumarin 153. are in most cases within this experimental error. However. all average solvation times measured with coumarin 152 are shorter than those measured with coumarin 153. which clearly indicates a small but noticeable probe dependence of the solvation dynamics.

3.3. The time dependence of the integrated emission intensity

The time-dependent Stokes shift of the fluorescence spectrum is not the only manifestation of transient solvation. The integrated emission intensity. emission polarization. and emission band shape also evolve during the solvation process [24]. In particular. the time dependence of the integrated emission intensity has received attention recently for solvation probes [25.26] and molecules that undergo excited state intramolecular electron transfer [21.27].

Figs. 2-4 show transient emission spectra for cou-
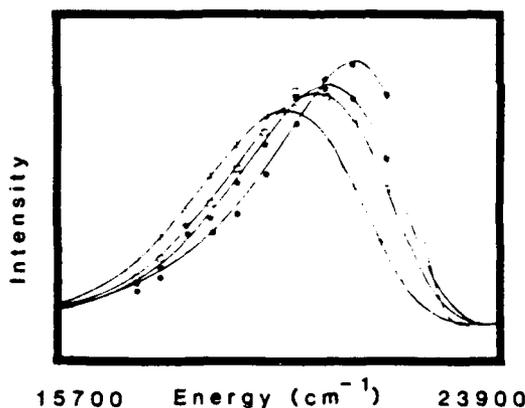
Fig. 3. Time-dependent fluorescence spectra of coumarin 152 in propylene carbonate obtained using the spectral reconstruction technique. The solid lines are log-normal fits to the data points which are denoted with ● (0.1 ps). ★ (0.5 ps). ☐ (1.0 ps). and ○ (5.0 ps).

11200 Energy (cm⁻¹) 25300
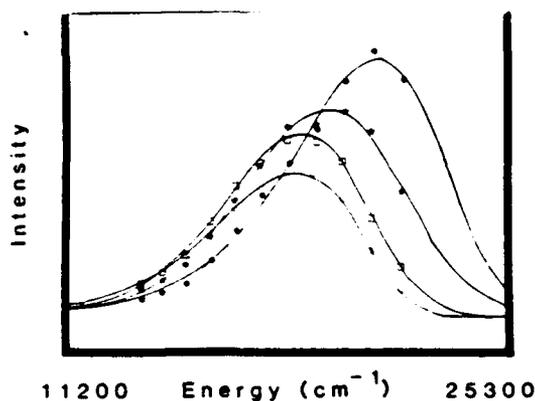
Fig. 4 Time-dependent fluorescence spectra of coumarin 153 in propanol obtained using the spectral reconstruction technique. The solid lines are log-normal fits to the data points which are denoted by ● (2.0 ps), ★ (30.0 ps), ☐ (100 ps), and ○ (400 ps).

marin 153 in propylene carbonate, coumarin 152 in propylene carbonate, and coumarin 153 in propanol. For the results in propylene carbonate, a small ($\approx 25\%$) but measurable drop in the integrated emission intensity is observed during the solvation process. This drop in intensity is not due to population decay, which is negligible on the time scale (5 ps) of figs. 2 and 3. The decrease of integrated area as solvation occurs and the fluorescence spectrum shifts toward lower frequency seems to parallel the situation for the *static* spectroscopy (of coumarin 152 and coumarin 153) [7,8,24], which gives a measure of the radiative and nonradiative properties of S_1 molecules in the presence of an equilibrated solvent configuration. It is observed that the radiative rate constant, k_n^0, which is proportional to the integrated emission intensity, decreases as the solvent polarity increases. Of course, as the solvent polarity increases, the emission maximum $\bar{\nu}(t=\infty)$ shifts toward lower frequency, so the overall effect is that the integrated emission intensity (correcting for loss due to population decay) decreases as the $\bar{\nu}(t=\infty)$ decreases, which is analogous to the time resolved observations (figs. 2 and 3). The situation is particularly dramatic for coumarin 153 in propanol as shown in fig. 4: the integrated emission intensity drops about 50% in the first 100 ps. It is unlikely that this decrease is due to

propanol is > 1 ns in this solvent.

The decrease in the integrated emission intensity as solvation occurs may be due to a variety of factors. Drops in integrated emission intensity of the magnitude reported here have been attributed to the fact that as the emission spectrum shifts to lower frequency, the radiative rate should decrease due to the ν^3 factor in the function relating the electronic part of the transition moment matrix element to k_n^0. On the other hand, large drops in integrated emission intensity during excited-state relaxation for excited-state electron transfer molecules like bianthryl have been attributed to an evolving electronic character of S_1 as the electron transfer occurs. If excited-state electron transfer plays some role for the coumarins, the effect is much less dramatic than bianthryl, which shows a time dependent decrease in the integrated emission intensity that is more than an order of magnitude larger then the coumarins [21]. Indeed, the fact that the integrated emission intensity decrease for the coumarins during solvation is not very large, is evidence that the coumarins are reasonably ideal solvation probes.

3.4. Comparison to dielectric continuum predictions

The simplest theoretical model for solvation is the uniform dielectric continuum model, which treats the solute as a cavity with a point dipole at the center, and the solvent as a uniform dielectric medium [3]. Employing this model, which we denote by DCM (dielectric continuum model), it is a straight forward task to calculate $C(t)$ from the frequency dependent dielectric response of the pure solvent. The situation is particularly simple for a Debye solvent, i.e. a solvent with an exponential dielectric response. In this case, $C(t)$ is predicted to be a single exponential with a relaxation time, τ_L, the longitudinal relaxation time, τ_L is given by

$$\tau_L = \frac{\epsilon_x}{\epsilon_s}\tau_D \qquad (2)$$

where ϵ_x, ϵ_s, and τ_D are the infinite-frequency dielectric constant, the static dielectric constant, and the dielectric relaxation time, respectively.

For other dielectric response functions, such as a multiple exponential response function, a Cole–Dav-

function. the predicted $C(t)$ is more complex than a single exponential decay. Nevertheless, $C(t)$ can be calculated for these various response functions within the DCM. As stated above. a comparison of experimental $C(t)$ data to predictions of $C(t)$ offers some information on the role of molecular scale processes and interactions in the solvation process. Simply stated. a large discrepancy between the observed $C(t)$ and the DCM predictions is evidence that the molecular interactions involved in the solvation process are very different from those involved in the dielectric relaxation of the pure liquid.
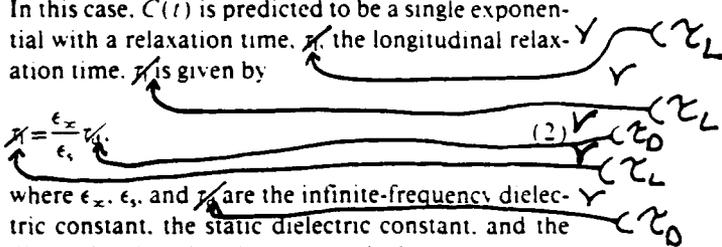
For the purpose of comparison of the experimental $C(t)$ data and the DCM predictions, we employ the following three characteristic relaxation times for $C(t)$:

(1) τ_i is the initial relaxation time which is calculated from the times in table 1 by

$$\tau_i = \frac{1}{A_1/\tau_1 + A_2/\tau_2};$$ (3)

(2) $\tau_{1/e}$ is the time required for $C(t)$ to decay to $1/e$;

(3) $0.5\,\tau_{1/e^2}$ is one half the time required for $C(t)$ to decay to $1/e^2$ [11].

Table 2 shows these values for the $C(t)$ data that was summarized in table 1. For a solvent with a single exponential $C(t)$. all three times (τ_i, $\tau_{1/e}$, and $0.5\,\tau_{1/e^2}$) should be identical. Experimentally. $C(t)$, for

gle exponential. The possible exception is acetone. for which a single exponential fit to $C(t)$ fits the data as well as a biexponential fit to $C(t)$ within experimental error, see table 2.

Dielectric relaxation data for most of the solvents in table 1 have been published. although the measurements have not been made at high enough frequency in all cases to ensure accurate characterization of the high-frequency response which is necessary to predict subpicosecond and femtosecond relaxation processes. As more accurate data become available at higher frequencies it will be possible to more accurately compare the DCM predictions and the experimental $C(t)$ data. The dielectric data used for our DCM predictions are summarized in table 3. Table 4 lists multiexponential fitting parameters for the DCM predicted $C(t)$. Table 5 lists the predicted $C(t)$ as the characteristic relaxation times τ_i, $\tau_{1/e}$, and $0.5\,\tau_{1/e^2}$.

It is remarkable how similar the average measured solvation time. $\langle \tau_s \rangle$. (table 1) is to the DCM prediction for this quantity (table 4) for the new measurements in various solvents. This is in general agreement with previous results that the DCM model accurately predicts the average time scale for solvation for a broad range of solvents [1-3,9,11]. For the solvents described in this paper. the predictions agree within a factor of two for all solvents except DMSO. for which the experimental values (for two different

Table 2

Experimentally determined initial inverse rates τ_i. $1/e$ relaxation times $\tau_{1/e}$. and 0.5 ($1/e^2$) relaxation times $0.5\,\tau_{1/e^2}$. For a more detailed description of these quantities. please refer to the text. Other abbreviations are the same as table 1

Solvent	Probe	Method	τ_i (ps)	$\tau_{1/e}$ (ps)	$0.5\,\tau_{1/e^2}$ (ps)
Propylene	C152	sr	0.83	1.68	2.34
carbonate	C152	lw	1.01	1.47	2.77
	C153	sr	0.89	2.03	4.05
	C153	lw	1.25	2.35	3.43
Propanol	C153	sr	25.6	29.8	33.3
DMSO	C152	lw	0.58	0.75	1.33
	C153	lw	0.63	1.04	1.57
Acetone	C152	lw	0.48	0.58	0.70
	C153	lw	0.83	0.83	0.83
DMF	C152	lw	0.60	0.77	1.04
	C153	lw	1.09	1.29	1.58
Water	DMACAA	sr	0.38	0.73	0.96
	C343	sr	0.40	0.49	0.64

Solvent	Dielec. model	parameters	Ref.
Propylene carbonate (293 K)	Cole–Davidson	$\epsilon_s=66.4$ $\epsilon_\infty=3.9$ $\tau_0=46.2$ $\beta=0.91$	[28]
ropanol (298 K)	Three component Debye	$\epsilon_s=20.6$ $\epsilon_{\infty1}=3.65$ $\epsilon_{\infty2}=3.03$ $\epsilon_{\infty3}=2.19$ $\tau_1=420$ $\tau_2=19.1$ $\tau_3=2.1$	[29]
DMSO (303 K)	Three component Debye	$\epsilon_s=47.1$ $\epsilon_{\infty1}=13.9$ $\epsilon_{\infty2}=4.84$ $\epsilon_{\infty3}=2.19$ $\tau_1=20.4$ $\tau_2=9.5$ $\tau_3=1.3$	[30]
DMF (303 K)	Three component Debye	$\epsilon_s=37.0$ $\epsilon_{\infty1}=17.6$ $\epsilon_{\infty2}=3.61$ $\epsilon_{\infty3}=2.46$ $\tau_1=12.8$ $\tau_2=6.9$ $\tau_3=0.7$	[30]
Acetone (293 K)	Debye	$\epsilon_s=21.20$ $\epsilon_\infty=1.90$ $\tau=3.3$	[31]

hand. perhaps the discrepancy between experiment and the DCM prediction is a harbinger of specific molecular interactions.

While the DCM model accurately predicts the average solvation time. it less accurately predicts the shape of $C(t)$. For example. we have previously shown that $C(t)$ for coumarin 152 in propylene carbonate decays more rapidly at early times than the DCM predicts. This can be seen by noticing that the experimental τ_s is much shorter than the DCM prediction for τ_s. The new results using coumarin 153 also exhibit this trend. This has been attributed to translational or librational motion of the solvent near the probe. which would not be present in the DCM prediction. On the other hand. the fact that the infinite frequency dielectric constant for propylene carbonate is so large ($\epsilon_\infty = 3.9$, obtained from the dielectric data) may indicate that the dielectric measurements actually missed a higher frequency component in the dielectric response. If such a component exists, its inclusion in a DCM prediction would cause an acceleration of the predicted $C(t)$ at early times. Once again. it would be useful to have new dielectric data on the solvent at higher frequency than has been recorded to date.

There is a very interesting discrepancy between the experimental $C(t)$ response of propanol and the DCM prediction for this solvent. namely the failure to observe in the experiment. the rapid initial decay which is predicted by the DCM calculations. The interpretation of the experiment is somewhat complicated by the details of how the transient data are collected. The transient emission data are recorded with a fixed time step for technical reasons. Unfortunately. this makes it difficult to study short decay

probes) are almost three times shorter than the DCM prediction. It would be useful to have new. higher frequency dielectric response data on this solvent in order to test whether the discrepancy is due to finite frequency response of the dielectric data. and conse-

Table 4

Dielectric continuum model calculations of solvation dynamics using the data from table 3

Solvent	τ_1 (ps)	τ_2 (ps)	τ_3 (ps)	$\langle\tau_s\rangle$ (ps)
Propylene carbonate	1.39 (50%)	3.83 (50%)	–	2.59
Propanol	74.4 (55.3%)	15.9 (13.7%)	1.52 (31.0%)	43.8
DMSO	6.02 (19.7%)	3.31 (52.4%)	0.96 (27.8%)	3.19
DMF	6.09 (7.9%)	1.42 (58.0%)	0.47 (34.2%)	1.47
Acetone	0.36	–	–	0.36
Water	0.48 (96%)	1.40 (4%)	–	0.52

Solvent	τ_i (ps)	$\tau_{1/e}$ (ps)	0.5 $\tau_{1/e}$ (ps)
Propylene carbonate	2.03	2.32	2.65
Propanol	4.54	33.7	52.4
DMSO	2.08	2.76	3.34
DMF	0.87	1.09	1.37
Acetone	0.36	0.36	0.36
Water	0.49	0.50	0.51

components in the presence of very long decay components because that would require a prohibitively large number of data points for a given transient. In order to circumvent this problem, we studied the emission dynamics of propanol on three different time scales, the shortest being about 1 picosecond. There is no evidence of an early, rapidly decaying component as predicted by the DCM model.

For the case of water the DCM prediction for $C(t)$ is nearly a single exponential. In contrast, the experimental data show a distribution of relaxation components, which has been discussed before [9]. It is important to note that the time resolution of the experiments described in this paper is roughly limited to greater than 100 femtoseconds. Solvation components with shorter time constants would not be resolved in these experiments. Unfortunately, molecular dynamics calculations on solvation in water and methanol predict that there should be significant decay components on a shorter time scale than we can resolve due to librational motion of the hydroxyl groups in the solvents [12,17]. In water the librational mode is particularly important, according to some of the simulations. But, even in linear alcohols it should play some significant role. Unfortunately, the experiments in this paper may offer little information on this type of relaxation.

3 5 Solvation dynamics of solvent mixtures

Transient solvation measurements of solvent mixtures is potentially a more stringent test of the dielectric continuum model since the environment in the vicinity of the fluorescent probe might have a very

than the solvent mixture in the absence of a probe. At present, dielectric data are only available for a few simple mixtures, and even for these mixtures, the dielectric data are restricted to a limited frequency range. The most favorable case is the binary solvent mixture acetonitrile–benzonitrile.

Emission transients for various mixtures, recorded at the so-called linear wavelength (see above), are shown in fig. 5. The best fit parameters of $C(t)$ and the characteristic relaxation times, obtained from the experimental transient solvation data of the mixtures and pure liquids, are given in tables 6 and 7.

Dielectric data for the various mixtures, the corresponding best fit parameters for $C(t)$, and the characteristic relaxation times are given in tables 7–10 respectively. The experimental data on pure benzonitrile agrees very well with the DCM predic-
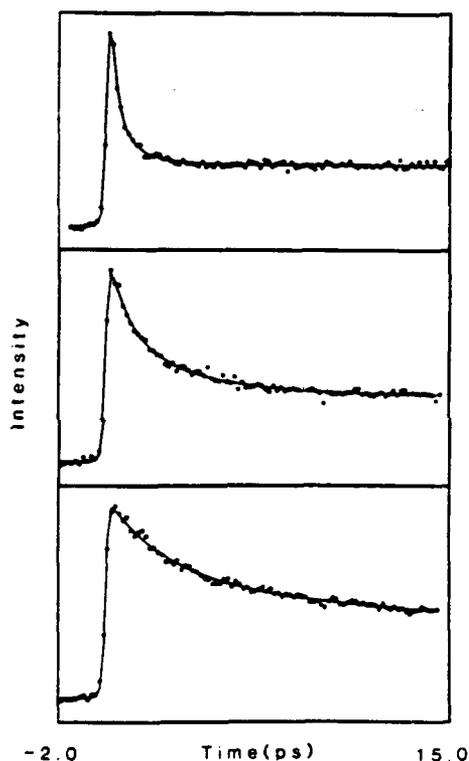
Fig. 5. Acetonitrile-benzonitrile transients using coumarin 152 as a probe and collecting at the "linear wavelength". The top frame is 100% acetonitrile, the middle frame is 66% benzonitrile, and the bottom frame is 100% benzonitrile.

Experimental solvation parameters for acetonitrile–benzonitrile mixtures measured with coumarin 152 as a probe molecule. X is the molar fraction of acetonitrile. τ_1, τ_2 are time constants of a biexponential fit to the transient solvation data. $\langle \tau_s \rangle$ is the average solvent relaxation time. All data were obtained using the linear wavelength method

X	τ_1 (ps)	τ_2 (ps)	$\langle \tau_s \rangle$ (ps)
0.0	2.3 ±0.5 (0.38)	8.2 ±2.0 (0.62)	5.3 ±0.7
0.31	1.2 ±0.3 (0.45)	4.5 ±0.2 (0.55)	3.0 ±0.2
0.54	0.6 ±0.4 (0.64)	4.5 ±2.3 (0.36)	2.0 ±0.7
0.73	0.27±0.12 (0.51)	1.4 ±0.4 (0.49)	0.82±0.29
0.88	0.3 ±0.1 (0.61)	1.3 ±0.4 (0.39)	0.69±0.05
1.0	0.27±0.09 (0.73)	1.05±0.35 (0.27)	0.48±0.1

Table 7

Experimentally determined initial inverse rates τ_i, $1/e$ relaxation times $\tau_{1/e}$, and 0.5 $(1/e^2)$ relaxation times 0.5 τ_{1/e^2} for acetonitrile–benzonitrile mixtures. X is the molar fraction of acetonitrile

X	τ_i (ps)	$\tau_{1/e}$ (ps)	$0.5 \, \tau_{1/e^2}$ (ps)
0.0	4.15	4.44	5.55
0.31	2.01	2.53	3.19
0.54	0.87	1.17	2.21
0.73	0.45	0.62	0.91
0.88	0.43	0.52	0.72
1.0	0.34	0.38	0.47

Table 8
Dielectric data for acetonitrile–benzonitrile mixtures

X	ϵ_0	ϵ_∞	τ_1 (ps)	τ_2 (ps)
0.00	25.6 [a]	3.85	33.0	–
	25.6 [b]	3.85	8.0	–
0.31 [c]	27.0	3.0	5.3 (30%)	32.5 (70%)
0.54	28.8	2.5	5.3 (54%)	33.0 (46%)
0.73	31.1	2.4	5.0 (73%)	24.2 (27%)
0.88	33.1	2.4	4.7 (88%)	12.0 (12%)
1.0 [d]	35.6	2.5	5.9	–

[a] Dielectric data from ref. [32] ($T=303$ K), with $\epsilon_\infty = 3.85$ taken from ref. [33].
[b] Dielectric data from ref. [33] ($T=294$ K).
[c] Dielectric data for mixtures from ref. [32] ($T=303$ K).
[d] Dielectric data from ref. [34] ($T=298$ K).

tion, in terms of average solvation time and shape of the $C(t)$ function, although the experimental data relaxes slightly more rapidly at early times. The pure acetonitrile data have an average experimental time

Dielectric continuum model calculations of solvation dynamics of acetonitrile–benzonitrile mixtures using the data in table 8

X	τ_1 (ps)	τ_2 (ps)	$\langle \tau_s \rangle$ (ps)
0.0	5.5 [a]	–	5.5
	1.3 [b]	–	1.3
0.31	1.45 (88%)	15.1 (12%)	3.1
0.54	0.84 (95%)	21.3 (5%)	1.9
0.73	0.57 (98%)	19.4 (2%)	0.95
0.88	0.44 (99.6%)	11.1 (0.4%)	0.48
1.0	0.47	–	0.47

[a] Dielectric data from ref. [32] ($T=303$ K), with $\epsilon_\infty = 3.85$ taken from ref. [33].
[b] Dielectric data from ref. [32] ($T=294$ K).

Table 10
Calculated (using the data in table 8) initial inverse rates τ_i, $1/e$ relaxation times $\tau_{1/e}$, and 0.5 $(1/e^2)$ relaxation times τ_{1/e^2} for acetonitrile–benzonitrile mixtures. X is the mole fraction of acetonitrile

X	τ_i (ps)	$\tau_{1/e}$ (ps)	τ_{1/e^2} (ps)
0.0	5.5 [a]	5.5	5.5
	1.3 [b]	1.3	1.3
0.31	1.63	1.76	2.16
0.54	0.88	0.91	0.99
0.73	0.58	0.59	0.61
0.88	0.44	0.44	0.45
1.0	0.47	0.47	0.47

[a] Dielectric data from ref. [32] ($T=303$ K), with $\epsilon_\infty = 3.85$ taken from ref. [33].
[b] Dielectric data from ref. [33] ($T=294$ K).

that is in agreement with the DCM prediction within experimental error, but there is apparently a broader distribution of relaxation times in the experimental $C(t)$ versus the DCM prediction, which is single exponential. This distribution can be seen by comparing the characteristic relaxation times, see tables 7 and 10.

The binary solvent mixtures show surprising agreement between experiment and DCM prediction, when the comparison is limited to the average relaxation time. The agreement is essentially within experimental error for the four mixtures and as stated above, there is also excellent agreement for the pure solvents. All solvent mixtures exhibit a broader dis-

Fig. 6. Temperature dependence of coumarin 153 in propylene carbonate at the "linear wavelength". The data in the top frame was obtained at 298 K and the data in the bottom frame was obtained at 267 K. The triangle in the bottom frame is an example of our instrument response function, used to fit the data.

tribution of relaxation times than predicted, see tables 7 and 10.

The broader distribution in the experimental data may be evidence of molecular structure near the probe but the effects are apparently not dramatic. It will be interesting to evaluate more microscopic theoretical models for the solvation dynamics in mixtures, as these models become available.

3.6. Variable temperature measurements

An interesting deviation from continuum predictions has been reported by Maroncelli and Fleming for propylene carbonate [24]. Employing the time-correlated single photon counting technique and the spectral reconstruction method of data analysis, these authors reported that the average solvation time was several times longer than the DCM prediction at lower temperatures for this solvent. Fig. 6 shows emission transients at the linear wavelength for coumarin 153 in propylene carbonate at 267 K and 298 K. The best fit parameters are summarized in table 11. It is interesting that there is an enormous spread in relaxation times for this solvent at the lower temperatures. For example, at 257 K, the different relaxation components range from the subpicosecond to the tens of picosecond time scale. Apparently, the earlier measurements failed to resolve the shortest time scale component that we report in this paper. In detail, the average solvation time we measure at 257 K is 14 picoseconds, while Maroncelli and Fleming report an average solvation time of 47 picoseconds at 252 K. Indeed, our new value is close to the prediction of the dielectric continuum theory.

In contrast to the results for coumarin 153 in propylene carbonate, coumarin 153 in propanol does not show a dramatic distribution of solvation times, see table 11. In this case our results agree with the slower time resolution results of Maroncelli and Fleming [24].

Table 11
The temperature dependence of solvation dynamics of propylene carbonate and propanol. In both cases the probe was C153 and the linear wavelength method was used

Solvent	T	τ_1 (ps)	τ_2 (ps)	τ_3 (ps)	$\langle \tau_s \rangle$ (ps)
Propylene carbonate	298	0.60 (40%)	4.6 (60%)	–	3.0
	267	4.7 (50%)	19 (50%)	–	12
	257	0.40 (14%)	3.7 (42%)	27.3 (44%)	14
Propanol	298	20 (40%)	63 (60%)	–	46
	291	30 (51%)	86 (49%)	–	58
	281	40 (59%)	148 (41%)	–	84
	273	59 (65%)	228 (35%)	–	118

4. Conclusions and summary

We have made new measurements on the dipolar relaxation of several new solvents and one binary solvent mixture in the presence of coumarin probes using femtosecond resolved fluorescence upconversion. In most cases, the dielectric continuum model accurately predicts the average solvation time, but often fails to predict the correct shape of the dipolar correlation function, $C(t)$. These results seem to hold at lowered temperatures and in a binary solvent mixture as well. This breakdown of the dielectric continuum theory is probably a manifestation of local motion of the solvent near the probe molecule, although the possibility that it is due to using incomplete dielectric data which does not accurately represent the high-frequency response of the solvent cannot be ruled out until better dielectric data become available. We also investigated the ideality of the coumarins as probes for dipolar relaxation and found, by comparing two different probes and by studying the integrated emission intensity as a function of time, that the possible complication due to twisted intramolecular charge transfer has only a small effect.

✶ correction

References

[1] J.D. Simon, Accounts Chem. Res. 21 (1988) 128.

[2] M. Maroncelli, J. MacInnis and G.R. Fleming, Science 243 (1989) 1674.

[3] P.F. Barbara and W. Jarzeba, Advan. Photochem. 15 (1990) 1.

[4] M.A. Kahlow, W. Jarzeba, T.P. DuBruil and P.F. Barbara, Rev. Sci. Inst. 59 (1988) 1098.

[5] E.W. Castner Jr., M. Maroncelli and G.R. Fleming, J. Chem. Phys. 86 (1987) 1090.

[6] G.C. Walker, W. Jarzeba, T.J. Kang, A.E. Johnson and P.F. Barbara, J. Opt. Soc. Am. B 7 (1990) 1521.

[7] M.A. Kahlow, W. Jarzeba, T.J. Kang and P.F. Barbara, J. Chem. Phys. 90 (1989) 151.

[8] M.A. Kahlow, T.J. Kang and P.F. Barbara, J. Chem. Phys. 88 (1988) 2372.

[9] W. Jarzeba, G.C. Walker, A.E. Johnson and P.F. Barbara, J. Phys. Chem. 92 (1988) 7039.

[10] B. Bagchi, Ann. Rev. Phys. Chem. 40 (1989) 115.

[11] M. Maroncelli, preprint.

[12] T. Fonseca, private communication.

[13] E.A. Carter and J.T. Hynes, J. Phys. Chem. 93 (1989) 2184 and references therein.

[14] J.S. Bader, R.A. Kuharski and D. Chandler, J. Chem. Phys. 93 (1990) 230.

[15] I. Rips, J. Klafter and J. Jortner, J. Chem. Phys. 88 (1988) 3246.

[16] D.F. Calef and P.G. Wolynes, J. Chem. Phys. 78 (1093) 4145;
A.L. Nichols III and D.F. Calef, J. Chem. Phys. 89 (1988) 3783.

[17] M. Maroncelli and G.R. Fleming, J. Chem. Phys. 89 (1988) 5044;
M. Maroncelli, E.W. Castner Jr., B. Bagchi and G.R. Fleming, Faraday Discussions Chem. Soc. 85 (1988) 1;
O.A. Karim, A.D.J. Haymet, M.J. Banet and J.D. Simon, J. Phys. Chem. 92 (1988) 3391.

[18] B. Bagchi, D.W. Oxtoby and G.R. Fleming, Chem. Phys. 86 (1984) 257.

[19] G. van der Zwan and J.T. Hynes, J. Phys. Chem. 89 (1985) 4181.

[20] V. Friedrich and D. Kivelson, J. Chem. Phys. 86 (1987) 6425;
M. Rao and B.J. Berne, J. Phys. Chem. 85 (1981) 1498;
R.F. Loring and S. Mukamel, J. Chem. Phys. 87 (1987) 1272;
R.F. Loring, Y.J. Yan and S. Mukamel, J. Phys. Chem. 91 (1987) 1302.
H.L. Friedman, J. Chem. Soc. Faraday Trans. II 79 (1983) 1465.

[21] T.J. Kang, M.A. Kahlow, D. Giser, S. Swallen, V. Nagarajan, W. Jarzeba and P.F. Barbara, J. Phys. Chem. 92 (1989) 6800;
T.J. Kang, W. Jarzeba, P.F. Barbara and T. Fonseca, Chem. Phys. in press.

[22] G. Jones II, W.R. Jackson and A.M. Halpern, Chem. Phys. Letters 72 (1980) 391;
G. Jones II, W.R. Jackson, C. Choi and W.R. Bergmark, J. Phys. Chem. 89 (1985) 294;
W. Rettig and A. Klock, Can. J. Chem. 63 (1985) 1649.

[23] V. Nagarajan, A.M. Brearley, T.J. Kang and P.F. Barbara, J. Chem. Phys. 86 (1987) 3183.

[24] M. Maroncelli and G.R. Fleming, J. Chem. Phys. 86 (1987) 6221.

[25] M. Maroncelli, preprint.

[26] N. Agmon, J. Phys. Chem. 94 (1990) 2959.

[27] J.D. Simon, private communication.

[28] E.A.S. Cavell, J. Chem. Soc. Faraday Trans. II 70 (1974) 78.

[29] E.W. Castner Jr., B. Bagchi, M. Maroncelli, S.P. Webb, A.J. Rugiero and G.R. Fleming, Ber. Bunsenges. Physik. Chem. 92 (1988) 363.

[30] N.M. Galiyarova and M.I. Shokhparanov, Fiz. Fiz. Khim. Zhidk. 4 (1980) 39.

[31] J. Calderwood and C.P. Smyth, J. Am. Chem. Soc. 78 (1956) 1295.

[32] J.K. Eloranta and P.K. Kabada, Trans. Faraday Soc. 66 (1970) 817.

[33] J.Ph. Poley, Appl. Sci. Res. B 4 (1955) 337.

[34] K.E. Arnold, J. Yarwood and A.H. Price, Mol. Phys. 48 (1983) 451.

TECHNICAL REPORT DISTRIBUTION LIST - GENERAL

Office of Naval Research (2)*
Chemistry Division, Code 1113
800 North Quincy Street
Arlington, Virginia 22217-5000

Dr. James S. Murday (1)
Chemistry Division, Code 6100
Naval Research Laboratory
Washington, D.C. 20375-5000

Dr. Robert Green, Director (1)
Chemistry Division, Code 385
Naval Weapons Center
China Lake, CA 93555-6001

Dr. Eugene C. Fischer (1)
Code 2840
David Taylor Research Center
Annapolis, MD 21402-5067

Dr. Elek Lindner (1)
Naval Ocean Systems Center
Code 52
San Diego, CA 92152-5000

Commanding Officer (1)
Naval Weapons Support Center
Dr. Bernard E. Douda
Crane, Indiana 47522-5050

Dr. Richard W. Drisko (1)
Naval Civil Engineering
 Laboratory
Code L52
Port Hueneme, CA 93043

Dr. Harold H. Singerman (1)
David Taylor Research Center
 Code 283
Annapolis, MD 21402-5067

Chief of Naval Research (1)
Special Assistant for Marine
 Corps Matters
Code 00MC
800 North Quincy Street
Arlington, VA 22217-5000

Defense Technical Information
 Center (2)
Building 5, Cameron Station
Alexandria, VA 22314

* Number of copies to forward

11